Aerodynamic Analysis of RQ-2 Fixed-Wing UAVs in Close Formation Flight

Joash Oendo and Naef Qasem

August 26, 2024

Aerodynamic analysis of RQ-2 fixed-wing UAVs in close formation flight

Joash M. Oendo, Naef A.A. Qasem

Abstract

Control and precision navigation advancements have renewed interest in formation flying for commercial and unmanned aerial vehicles (UAVs). Most of the research in this area has focussed on extended formation flying, which is unsuitable and less effective for UAVs. Various bioinspired formation patterns, including the echelon, normal V, and inverted V patterns, have been proposed for research and use in the aviation industry. The optimal separation distance is maintained for maximum aerodynamic benefits of flying. Formation controllers, in conjunction with wake and vortex tracking sensors, can be used to achieve this and maintain the preferred formation pattern and structure. This research examined the effects of close formation flying on the lift, induced drag, and, consequently, the overall range of UAVs. The aerodynamic benefits of flying UAVs in coordinated formation patterns included reduced drag and increased lift by positioning the trailing UAVs at optimal longitudinal, lateral, and vertical separation distances behind the leading UAVs. A lift/drag ratio increase of 25.6% and 52.4% were achieved in the inverted V and the normal V pattern, respectively. This corresponded to an average increase of 8.5% and 17.4% in the capable range of the UAV. The typical V-formation pattern proved better than the inverted V pattern due to the reduced induced adverse rolling effect on the trailing UAV on the former formation pattern.

Peer-review under responsibility of the scientific committee of the 24th EURO Working Group on Transportation Meeting.

Keywords: V-formation Flight; UAVs; Aerodynamics Performance; Rolling Effect; Vortex

1. Introduction

Unmanned aerial vehicles (UAVs) are best defined as aircraft designed to fly with no human controller (e.g., pilot) on board (Mohsan et al., 2023). The United States Office of the Secretary of Defense (Miller & Chadwick, 2018) takes the definition a step further, including the idea that they fly without a human controller on board and can also fly autonomously or be remotely piloted. UAVs use aerodynamic forces to provide lift for the aerial vehicle; they can be considered expendable or recoverable, and they can carry a lethal payload (as found in military use) or a non-lethal payload (as seen in commercial and civilian use). There are various classes of UAVs (Ps & Jeyan, 2020), including rotorcraft UAVs and fixed-wing UAVs, each with their advantages and disadvantages, whereby fixed-wing UAVs are preferred in long-range flights. However, their flight range is limited mainly due to low battery storage capacity; thus, these fixed-wing UAVs need to increase their capable range.

The use of formation flight on aircraft and UAVs shows momentous potential in increasing the capable range and improving the efficiency of task execution, among other benefits (Qiao et al., 2024). The idea of formation flight is a bioinspired concept that seeks to utilize the updraft air caused by the wing tip vortex effect of the leading aircraft or UAV in coordinated close formation, which has a significant impact on the aerodynamic characteristics of the trailing aircraft, including increase in lift and reduction in drag (Cai et al., 2012).

Aircraft formation flying and wake surfing are inspired by migratory birds, such as the Spruce geese, that fly in close formations, which increases their range by up to 71% for long solo flights (Corcoran & Hedrick, 2019). The concept involves aircraft taking off separately and climbing to the desired cruise altitude before being coordinated into a close formation flight pattern, with interchangeable roles as the lead and follower aircraft during the entire cruise phase. The follower aircraft are maintained at a particular vertical and longitudinal separation distance aft of the leader and optimal wingtip spacing or separation distance. The wingtip vortices of the leading aircraft create a smooth current of rotating air behind, flowing upwards and downwards in the outer and inner sections of the vortices, respectively. The outer side of the vortex is known as the updraft air, which causes an increase in lift in the follower aircraft (Gerz et al., 2002). There is also a relatively lower pressure gradient between the front and rear projected surfaces of the follower aircraft, reducing drag.

A pilot or an Autopilot stabilizes the follower aircraft in the updraft air to take advantage of the reduced drag and increased lift. The engine power of the follower can be reduced, therefore reducing fuel consumption. This increases the capable range of the trailing aircraft. This can technically be called wake surfing or wake energy retrieval (Lv et al., 2016).

Fixed-wing UAVs, and UAVs in general, have limited usage in long-range missions and operations due to their limited capable range because of low battery capacity (for electric-powered UAVs) and low fuel storage capacity (for engine-powered UAVs) as well as limited maximum load capacity owed to their compact design (Mohsan et al., 2023). Therefore, fixed-wing unmanned aerial vehicles can utilize wake surfing in formation flight to increase their range. A noble example of such is the reference UAV used for this analysis, the Pioneer RQ-2 UAV.

The Pioneer RQ-2 UAV (Williams, 2004) was developed by the AAI Corporation. The RQ-2 is an autonomous fixed-wing UAV with a length and wingspan of 4.3m and 5.1m, respectively, and a gross weight of 205kg. It has an optimum cruise speed of 30m/s, a range of 185km, and an endurance of 5 hours. The UAV is designed to carry a variety of payloads to perform missions such as reconnaissance, surveillance, and cargo transport (Durmaz et al., 2023).

This paper is organized as follows: Section 2 outlines the current work, summarizing the existing knowledge and progress. Section 3 explains the proposed methodology, including the aerodynamic analysis carried out in this research. In Section 4, the results and discussions of the analysis are showcased, and lastly, Section 5 gives the conclusions of the study limitation and suggests possible directions for further research.

2. Literature Review

Various formation patterns have been proposed for analysis to capitalize on the benefits of formation flying. The main types of formations include the normal V, inverted V, and echelon patterns (Cai et al., 2012). The benefits and challenges of formation flying for aerodynamics benefits were studied by Halaas et al. (2014) for the Air Force Research Lab and DARPA. Aircrafts flying in formations, with separation distances of between 3000 and 8000 feet, were analyzed using both CFD simulations and flight tests for comparison and validation. An increase of up to 15% was observed in the Lift-drag ratio of the trailing aircraft. The document served as a detailed reference for simulations on fixed-wing aircraft in formation flight.

Zhang et al. (2018) conducted a detailed numerical analysis of the aerodynamic characteristics of three tailless UAVs in close formation flight. The simulation aimed to facilitate a greater understanding of vortex effects between tailless UAVs and to back the technical applications of various close-formation flights technically. Normal V, inverted V, and echelon formations were analyzed to determine the aerodynamic benefits of optimum separation distances. Finite volume solver software CFX 15.0 was utilized for all the analysis simulations, with the standard k-Ɛ as the turbulence model used. A simplified tailless delta-wing UAV model CT-1 was modeled (Subash et al., 2024), and its aerodynamic characteristics were determined. Various longitudinal, lateral, and vertical separation distances were analyzed to determine the increase in lift and drag reduction and the optimal positioning for the trailing UAV. It was determined that there was an increase in the lift-drag ratio of the trailing UAVs by up to 25.4% and that it was dependent on the positioning of the UAVs (Zhang et al., 2018).

A novel idea discussed in this paper is the use of formation flight for fixed-wing UAVs flying on a similar path during a particular time-scheduled period. The UAVs are organized in interchangeable roles as lead and follower UAV, which enjoys increased lift and reduced drag because of the updraft air caused by the vortices of the lead UAV (Bangash et al., 2006). There is limited research and literature on formation flight for fixed-wing UAVs, and the few analyses in the current literature consider only ideal cases of basic simplified models. With the aim of further increasing the range of long-range fixed-wing UAVs and generating the necessary data required for developing robust control systems with innate capabilities such as vortex tracking to facilitate formation flight for fixed-wing UAVs, this paper deals with aerodynamic analysis on RQ-2 fixed-wing UAVs in formation flight during cruise phase.

3. Methodology

The geometry of the RQ-2 UAV was carried out using SOLIDWORKS Software. Manufacturer dimensions and specifications were used to model the UAV to scale. The main specifications include a length of 4.3m, wing cord length, and wingspan of 0.54m and 5.1m, respectively, as the Pioneer RQ-2 UAV general specifications (Md Abir, 2022). Then, the aerodynamic characteristics of this model during the cruise phase were analyzed using ANSYS Fluent Software. Fig. 1 below shows the proposed methodology and the designed model used in this analysis.

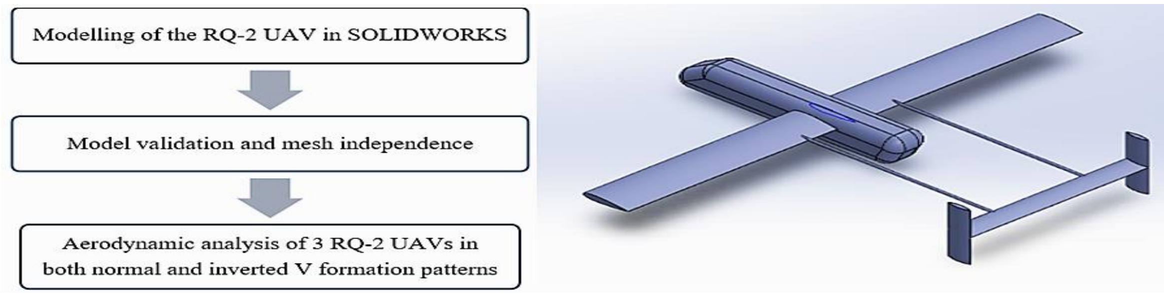

Fig. 1. The flow chart of the proposed methodology (left side) and the isometric view of the design model of the RQ-2 UAV (right side).

3.1 Model validation

The validation of the numerical results against the experimental data (Robert M, 1991) for drag coefficient, lift coefficient, and pitching moment, respectively, shows an excellent agreement between the results.
The acquired results were compared to experimental data on a wind tunnel test. The experimental study was carried out on a 0.4 scale RQ-2 UAV model in a low-speed wind tunnel at Wichita University. The tests were run on a 7 by 10 feet wind tunnel and a chord length based on a Reynolds number of 1.06×10^6.

Fig. 2 compares and validates the present model results against the experimental data of Robert M. (1991).

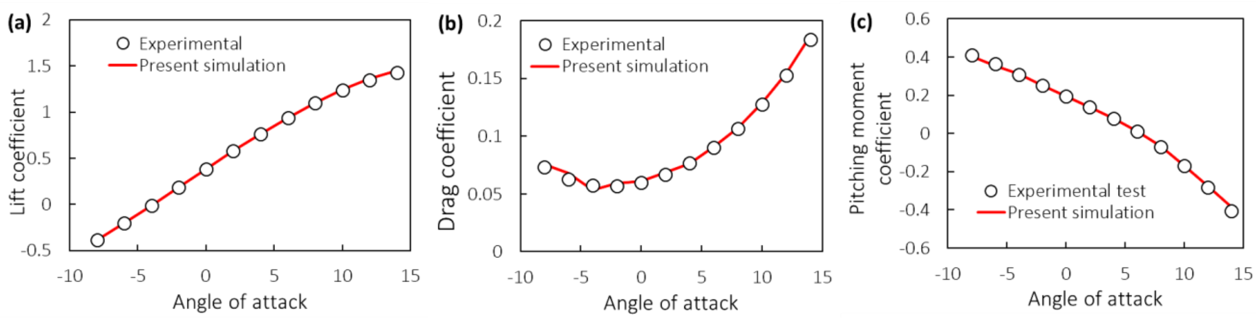

Fig. 2. Validation of the present model vs the experimental data of Robert M. (1991) in terms of (a) lift coefficient, (b) drag coefficient, and (c) pitching moment coefficient.

3.2 Mesh independence

Mesh independence is conducted among different mesh numbers to ensure no biased effect on the results from the meshing scheme. Starting with more than 800,000 cells and going up to 1500,000 cells, the lift coefficient does not change, as shown in Fig. 3. Thus, any mesh with > 800,000 cells is acceptable. The mesh scheme is shown in Fig. 3.

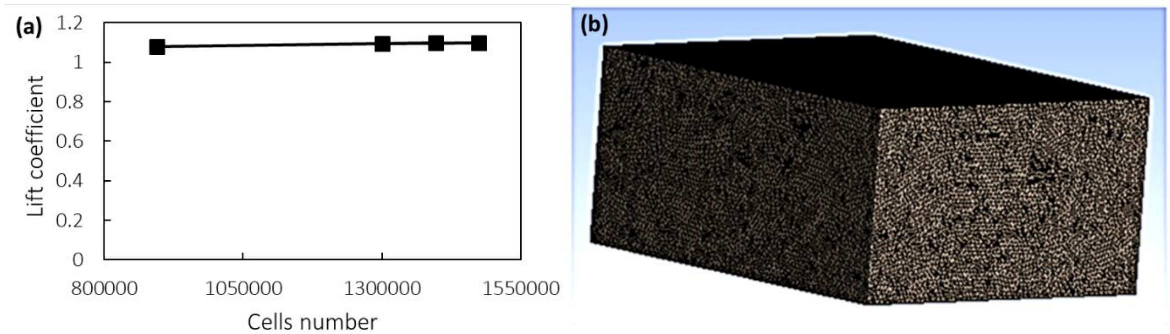

Fig. 3. (a) Mesh independence used in terms of lift coefficient and (b) final refined flow domain mesh.

3.3 Aerodynamic analysis of RQ-2 UAV

Figure 4 represents the inverse and normal V-formation studied in this research, respectively.

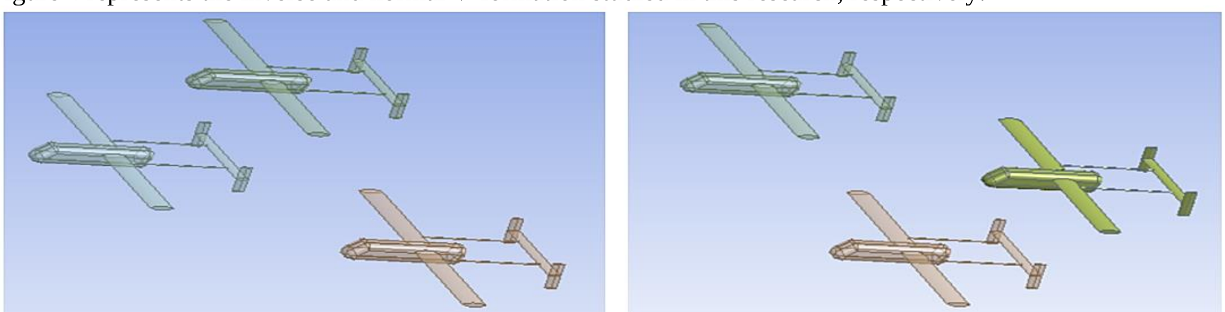

Fig. 4. Inverted V pattern geometry (left side) and normal V pattern geometry (right side).

4. Results and discussion

Streamwise growth of the vortices was used as the main factor to determine the optimum longitudinal separation distance. The trailing UAV should be close enough to enjoy the aerodynamic benefits of flying in the upwash air of the leading UAV but far enough to experience a balanced upwash effect on both wings, reducing the adverse rolling moment. The interaction between the wing tip vortices and the tailplane flow results in a large elliptical-shaped vortex, as can be seen in the figures below, showing the vorticity contours for the airflow behind the leading UAV at cross-sectional planes located 5 m and 10 m downstream.

Fig. 5(a) shows vorticity contours at a plane 5 m behind the leading UAV. The flow past the leading UAV model is highly rotational. This is demonstrated by the high rotational velocity gradient between the vortex core and outer regions in the figure below. This would result in a high-rolling moment on the trailing UAV. Fig. 5(b) shows vorticity contours at a plane 10 m from the leading UAV model; the flow is less rotational due to the decrease in the intensity of the vortices. The flow on the outer regions of the vortex formed a slow mass of rotating updraft air (the turquoise-colored region) with a lower gradient rotational velocity gradient. A UAV flying in this updraft region at 10m would experience fewer rolling moments than 5m.

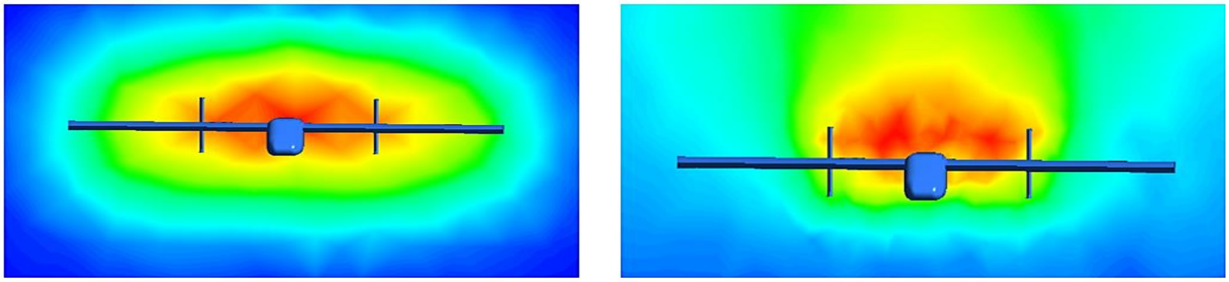

(a) (b)

Fig. 5. (a) Vorticity contours at a plane 5 m behind the leading UAV and (b) vorticity contours at a plane 10m behind the leading UAV.

The vertical separation affects the rolling moment acting on the trailing UAV because of the pronounced lateral velocity component near the top and bottom regions of the vortex. Fig. 6 below shows the vorticity contours on horizontal planes at various vertical separation distances.

Fig. 6(a) shows the vortex region at a horizontal plane -0.25 m vertical separation. The vortex core region size is relatively larger and close to the UAV fuselage section. In Fig. 6(b), the vortex core and region grow with longitudinal and vertical separation distance, forming a large desirable region of smooth rotating mass of updraft air (shown in turquoise color) downstream at a vertical separation distance of -0.5 m.

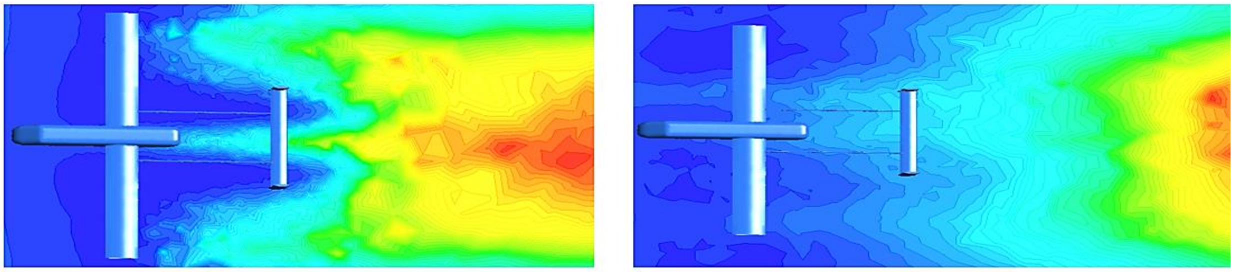

(a) (b)

Fig. 6. (a) Vortex region at a horizontal plane at a vertical separation distance of -0.25 m and (b) vortex region at a horizontal plane at a vertical separation distance of -0.5 m.

Fig. 7(a) shows a relatively smaller distribution due to the reduced size of the vortex due to the reduced separation distance. Fig. 7(b) shows a gradual increase in the vortex size with the increase in the separation distance, and Fig. 7(c) shows a gradual increase in vortex size with the increase in the longitudinal and lateral separation distance. This results from the growth in size with an increase in the longitudinal distance, increasing the width of the vortex and vortex core. A downward spread and shift in the vortex region and core were also noted, as shown in Fig. 7.

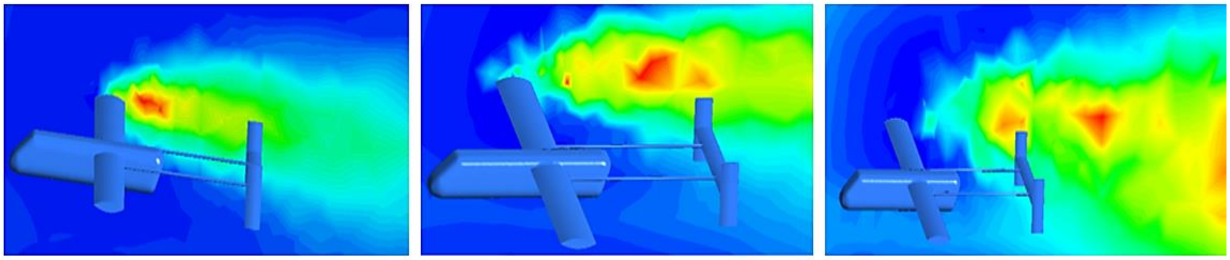

(a) (b) (c)

Fig. 7. (a) Plane at the right wing tip 2.5 m lateral separation distance, (b) plane at the right wing tip 3 m lateral separation distance, and (c) plane at the right wing tip 3.75 m lateral separation distance.

The velocity contours on the trailing UAV were also determined in this research. Fig. 8(a) shows velocity contours on the wings of the normal V pattern trailing UAV. The highest vertical velocity component of about 17.18 m/s on the UAV surface was experienced on the lower fuselage and wing sections and the fuselage lower leading edge section of the fuselage. The lowest vertical component of the airflow around the UAV surface, about -14.18 m/s, was experienced around the trailing edge sections of the wing and fuselage as a result of the airflow acceleration due to the curvature or shape of these surfaces. Fig. 8(b) shows the velocity magnitude contours on the trailing UAV in close formation flight. The velocity magnitude contour shows a more balanced distribution on both sides of the UAV. The highest velocity of 41.23 m/s is experienced on the airflow above the wing surface and some parts of the tailplane and fuselage forward section. The lowest velocity of 0m/s was experienced on the fuselage leading section where there is a point of airflow stagnation.

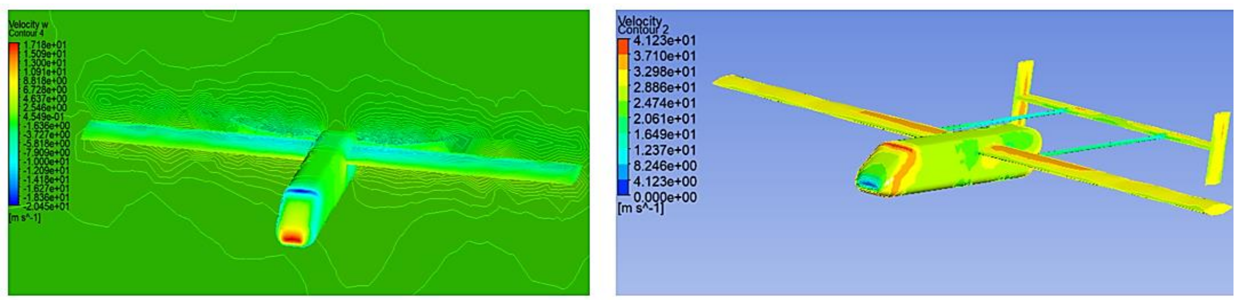

(a) (b)

Fig. 8. (a) A balanced velocity contour of the normal V pattern trailing UAV wings and (b) velocity magnitude contours on the trailing UAV surface.

In Fig. 9(a), the curve shows the Lift/Drag (L/D) ratio variation as a percentage of the reference L/D ratio for a single UAV in solo flight at different lateral separation distances. There was a notable decrease in the lift coefficient and lift-to-drag ratio at a lateral separation distance of about 24.7% and 20.57%, respectively. This decrease is a result of the downwash effect on one UAV wing. The lift and lift drag ratio is optimum at a lateral separation distance of 3.75m at a 24.4% increase, where the entire UAV experiences an upward velocity component due to the upwash effect in the outer segment of the vortex.

In Fig. 9(b), the curve shows the lift/drag ratio variation with the vertical separation distances. An increase of 21.69% in the lift coefficient was observed at the -0.5 m vertical separation distance compared to the 23.22% and 12.34% increase for the 0 and 0.5m separation distances. Only a slight reduction of 1% to 3.6% of the drag coefficient was observed. A 13% to 26% increase in lift/drag ratio was observed compared to the ratio for a single UAV on a solo flight. Fig. 9(c) shows variations in pitching and rolling moments with various vertical separation distances. A minimal variation of about 2% to 4% was observed with variation in the vertical separation distance for the pitching moment, while the change in the rolling moment could reach 26%. This is because of the pronounced lateral velocity component near the top and bottom regions of the vortex.

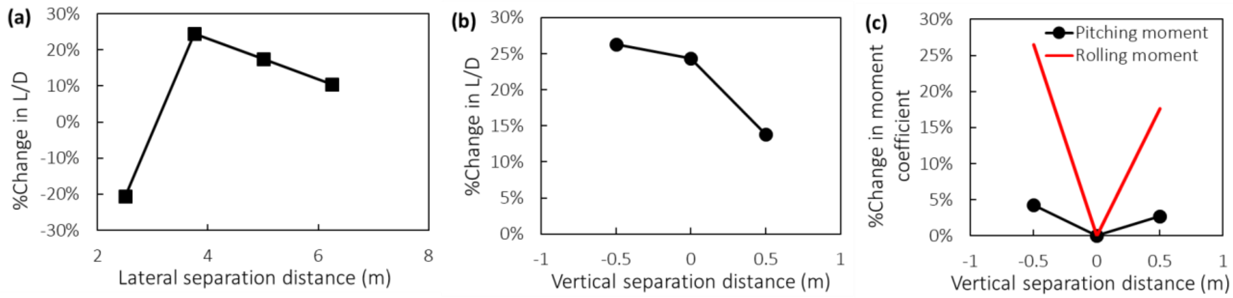

Fig. 9. (a) Percentage variation in L/D ratio with lateral separation distance, (b) Percentage variation in L/D ratio with vertical separation distance, and (c) Variation in pitching and rolling moments with vertical separation distance.

Fig. 10 displays the aerodynamic characteristics of the UAVs in inverse V and normal V close formation flight patterns, respectively. Fig. 10(a) shows a notable increase in the lift, pitching, and rolling moment coefficients on the trailing UAVs. A slight reduction in the drag coefficient was also noted, and a 25.6% increase in the lift/drag ratio was also noted on the trailing UAVs. This translated to an average increase of 8.5% in the range UAV-capable. In Fig. 10(b), which shows the aerodynamic characteristics of the normal V pattern, there is a notable increase in the lift coefficient and pitching moment coefficient on the trailing UAVs. A slight reduction in the drag coefficient was also noted, and a 52.4% increase in the lift/drag ratio was also noted. This translated to an average increase of 17.4% in the UAV-capable range. The rolling moment for the normal V-formation pattern was lower than for the inverted V-formation pattern due to the more balanced up-wash effect on both UAV wings.

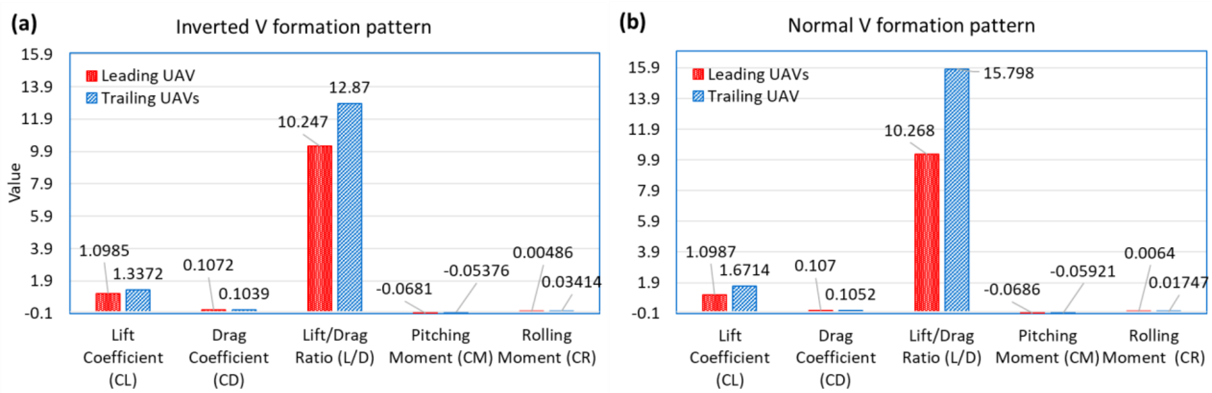

Fig. 10. (a) Aerodynamic characteristics of the UAVs (a) in inverted V pattern and (b) in normal V pattern.

5. Conclusions

This study demonstrates that the coordinated close formation flight for SMR UAVs can improve the aerodynamic characteristics, such as increasing the lift/drag ratio, which increases the UAV's total range. The aerodynamic benefits of flying UAVs in coordinated formation pattern, such as reduction in drag as well as increase in lift and lift/drag ratio, could be increased by positioning the trailing UAV(s) at optimal longitudinal, lateral, and vertical separation distances behind the leading UAV(s). The main contribution to the increase in the lift/drag ratio on the trailing UAV, as determined by the analysis, was the increase in the lift coefficient. The increase in the drag was minimal, in the range of 3% to about 7% of that of a UAV in solo flight. Some increased components of pitching and rolling moments were induced by flying in formation. This, however, could be counteracted by minimal deflections of the elevators and the ailerons, respectively. In the normal V pattern, the pitching moment can be corrected by an elevator deflection of between 2^{o} to 3^{o}, and the rolling moment by an aileron deflection of about 7^{o} while in the inverted V pattern, the pitching moment can be countered by an elevator deflection of about 2^{o} to 3^{o} and the rolling moment by an aileron deflection of 15º to 20º as determined from the control parameters of the RQ-2 UAV. The normal V formation pattern proved to be better than the inverted V pattern due to the reduced induced adverse rolling effect on the trailing UAV on the former formation pattern. The reduced adverse rolling moment in the normal v formation pattern is a result of the more balanced updraft effect from the leading UAV vortices on both wings of the trailing UAV. However, full and experimental aerodynamic analysis on the entire UAV is beyond the scope of this study as it is only numerical. Full aerodynamic analysis and wind tunnel tests on UAVs in formation flight could be done further to develop research data and knowledge in this area. In conclusion, this study's results can serve as a comprehensive reference for further research on formation flying for aerodynamic benefits for fixed-wing UAVs.

Acknowledgements

The authors thank the Department of Aerospace Engineering, KFUPM, for supporting this research.

References

Bangash, Z. A., Sanchez, R. P., Ahmed, A., & Khan, M. J. (2006). Aerodynamics of Formation Flight. *Journal of Aircraft*, *43*(4), 907–912. https://doi.org/10.2514/1.13872

Cai, D., Sun, J., & Wu, S. (2012). UAVs Formation Flight Control Based on Behavior and Virtual Structure. In T. Xiao, L. Zhang, & M. Fei (Eds.), *AsiaSim 2012* (Vol. 325, pp. 429–438). Springer Berlin Heidelberg. https://doi.org/10.1007/978-3-642-34387-2_49

Corcoran, A. J., & Hedrick, T. L. (2019). Compound-V formations in shorebird flocks. *eLife*, *8*, e45071. https://doi.org/10.7554/eLife.45071

Durmaz, M., CiCi, K., Sarikaya, M., BiLiCi, M., & BiLgiÇ, H. H. (2023). Metaheuristic algorithm-based cascade PID controller design for fixed wing unmanned aerial vehicle. *European Mechanical Science*, *7*(4), 230–237. https://doi.org/10.26701/ems.1243796

Gerz, T., Holzäpfel, F., & Darracq, D. (2002). Commercial aircraft wake vortices. *Progress in Aerospace Sciences*, *38*(3), 181–208. https://doi.org/10.1016/S0376-0421(02)00004-0

Halaas, D. J., Bieniawski, S. R., Whitehead, B., & Blake, W. B. (2014, January 13). Formation Flight for Aerodynamic Benefit Simulation Development and Validation. *52nd Aerospace Sciences Meeting*. 52nd Aerospace Sciences Meeting, National Harbor, Maryland. https://doi.org/10.2514/6.2014-1459

Lv, P., Rao, A. G., Ragni, D., & Veldhuis, L. (2016). Performance Analysis of Wake and Boundary-Layer Ingestion for Aircraft Design. *Journal of Aircraft*, *53*(5), 1517–1526. https://doi.org/10.2514/1.C033395

Md Abir. (2022). *Numerical Investigation of a Fixed Wing Mini UAV*. https://doi.org/10.13140/RG.2.2.35294.92480

Miller, C., & Chadwick, S. (2018). *Military Unmanned Aerial Vehicles and Diversification Opportunities*. https://doi.org/10.13140/RG.2.2.25777.02402

Mohsan, S. A. H., Othman, N. Q. H., Li, Y., Alsharif, M. H., & Khan, M. A. (2023). Unmanned aerial vehicles (UAVs): Practical aspects, applications, open challenges, security issues, and future trends. *Intelligent Service Robotics*. https://doi.org/10.1007/s11370-022-00452-4

Ps, R., & Jeyan, M. L. (2020). Mini Unmanned Aerial Systems (UAV)—A Review of the Parameters for Classification of a Mini UAV. *International Journal of Aviation, Aeronautics, and Aerospace*. https://doi.org/10.15394/ijaaa.2020.1503

Qiao, N., Ma, T., Wang, X., Wang, J., Fu, J., & Xue, P. (2024). An approach for formation design and flight performance prediction based on aerodynamic formation unit: Energy-saving considerations. *Chinese Journal of Aeronautics*, *37*(3), 77–91. https://doi.org/10.1016/j.cja.2024.01.002

Robert M, B. (1991). *A wind tunnel study of the Pioneer remotely piloted vehicle* [Wichita State University]. https://hdl.handle.net/10945/43784

Subash, Prof. T., Mayank, M. M., Srikanth, G., G, S., & Nd, G. (2024). Literature Study on Tailless UAV. *IARJSET*, *11*(3). https://doi.org/10.17148/IARJSET.2024.11316

Williams, K. (2004). *A Summary of Unmanned Aircraft Accident/Incident Data: Human Factors Implications*. 17.

Zhang, D., Chen, Y., Dong, X., Liu, Z., & Zhou, Y. (2018). Numerical Aerodynamic Characteristics Analysis of the Close Formation Flight. *Mathematical Problems in Engineering*, *2018*, 1–13. https://doi.org/10.1155/2018/3136519